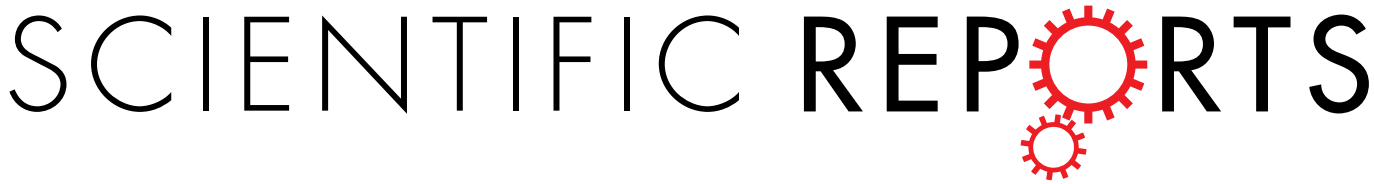

OPEN

Determination of magnetic anisotropy constants and domain wall pinning energy of Fe/MgO(001) ultrathin film by anisotropic magnetoresistance

Received: 25 March 2015
Accepted: 23 July 2015
Published: 15 September 2015

Bo Hu, Wei He, Jun Ye, Jin Tang, Yong-Sheng Zhang, Syed Sheraz Ahmad, Xiang-Qun Zhang & Zhao-Hua Cheng

It is challenging to determine domain wall pinning energy and magnetic anisotropy since both coherent rotation and domain wall displacement coexist during magnetization switching process. Here, angular dependence anisotropic magnetoresistance (AMR) measurements at different magnetic fields were employed to determine magnetic anisotropy constants and domain wall pinning energy of Fe/MgO(001) ultrathin film. The AMR curves at magnetic fields which are high enough to ensure the coherent rotation of magnetization indicate a smooth behavior without hysteresis between clockwise (CW) and counter-clockwise (CCW) rotations. By analyzing magnetic torque, the magnetic anisotropy constants can be obtained. On the other hand, the AMR curves at low fields show abrupt transitions with hysteresis between CW and CCW rotations, suggesting the presence of multi-domain structures. The domain wall pinning energy can be obtained by analyzing different behaviors of AMR. Our work suggests that AMR measurements can be employed to figure out precisely the contributions of magnetic anisotropy and domain wall pinning energy, which is still a critical issue for spintronics.

The magnetic properties of Fe film epitaxially grown on MgO(001) substrate have attracted much attention since the discovery of a very high tunneling magnetoresistance ratio in Fe/MgO/Fe magnetic tunneling junction[1–3]. It is well known that the magnetization switching process of Fe/MgO(001) is crucial for spintronic applications[4]. Although Fe(001) film usually exhibits an intrinsically in-plane four-fold magnetocrystalline anisotropy, an additional uniaxial magnetic anisotropy (UMA)[5] is always superimposed on the magnetocrystalline anisotropy owing to the surface steps of substrates[6], oblique deposition[7] or dangling bonds[8]. Depending upon the orientation of the applied field and the strength of UMA, the UMA profoundly affects the magnetization switching process, leading to "one-jump", "two-jump" or other types of magnetic hysteresis loop[9,10]. When the ratio of the four-fold magnetic anisotropy constant K_1 and UMA constant K_U, $K_U/K_1 < 1$, two-jump magnetization switching process will appear in the hysteresis loops of Fe(001)/MgO(001) film[9]. The two-jump magnetization switching process can be explained by competition of the 90° domain wall pinning energy and magnetic anisotropy energy[11,12].

A fundamental understanding of the evolving magnetic anisotropy and domain wall pinning energy remains elusive and is still a critically technological issue because they determine the magnetization switching process and the dynamic response on nanoscale[13,14]. The domain wall pinning energy and magnetic anisotropy can be separately investigated by various experimental methods[9,15,16]. Unfortunately,

State Key Laboratory of Magnetism and Beijing National Laboratory for Condensed Matter Physics, Institute of Physics, Chinese Academy of Sciences, Beijing 100190, China. Correspondence and requests for materials should be addressed to Z.-H.C. (email: zhcheng@iphy.ac.cn)

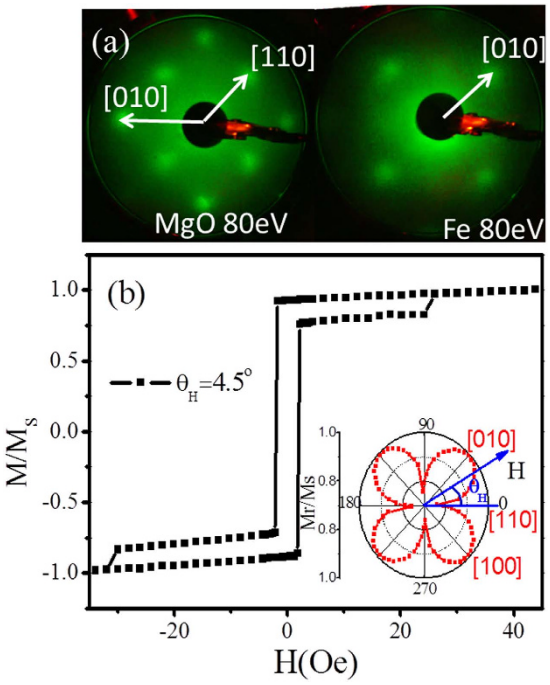

Figure 1. The typical LEED patterns of the substrate and sample, and MOKE measurement. (**a**) The typical LEED patterns of MgO(001) substrate and Fe(001) films, (**b**) The hysteresis loop of Fe/MgO(001) measured at $\theta_H = 4.5°$ near hard axis by MOKE measurement. The inset indicates the angular dependence of M_r/M_S and direction of Fe film hard and easy axes.

it is challenging to investigate the domain wall pinning energy and magnetic anisotropy of Fe/MgO(001) film simultaneously by a single method since both coherent rotation and domain wall displacement coexist during magnetization switching process.

In this paper, the angular dependence anisotropic magnetoresistance (AMR) measurement was introduced to investigate magnetization switching process in Fe(001) film on MgO(001) substrate. By carefully analyzing angular dependence AMR at high fields and low fields, the magnitudes of additional UMA and four-fold magnetic anisotropy constants as well as the values of domain wall pinning energy can be obtained, respectively. The contributions of magnetic anisotropy and domain wall pinning energy of Fe/MgO(001) film can be probed precisely by AMR measurements in our work.

Results

As shown in the left panel of Fig. 1(a), the typical low-energy electron diffraction (LEED) pattern indicates a clean MgO(001) substrate surface. Due to the relatively small lattice mismatch of Fe(001)||MgO(001) and Fe[100]||MgO[110] (3.8%)[17], the Fe(001) layers grow epitaxially with *bcc* lattice structure on the MgO(001) surface. A tetragonal distortion results in epitaxial relationship between Fe layer and MgO substrate in 45° in-plane rotation[7,18]. The good quality of Fe film is also verified by *in-situ* LEED pattern (right panel of Fig. 1(a)). The hysteresis loop of Fe/Mg(001) film characterized by longitudinal magneto-optical Kerr effect (MOKE) exhibits two-jump magnetization switching process, which can also be observed in other literature in the case of $K_U/K_1 < 1$[9]. Moreover, angular dependence M_r/M_S as shown in the inset of Fig. 1(b) indicates four-fold magnetic anisotropy of film. From the LEED pattern and in-plane MOKE analysis, Fe[110] and [100] axes can be confirmed as shown in Fig. 1(a).

The two-jump magnetization switching process is related to the K_1 and K_U. In order to figure out those parameters, the angular dependence AMR at high field of 730 *Oe* was measured as shown in Fig. 2(a). The AMR can be expressed as Eq. (1)[16,19–23]:

$$R_{XX} = R_\perp + \left(R_{//} - R_\perp\right)\cos^2(\theta_M - \alpha) \quad (1)$$

where θ_M and α are angles of magnetic moment M and current I measured from the Fe[110] direction. The current was applied at an angle $\alpha = 6.3°$ with respect to Fe [110] for AMR measurements, which will be discussed in details later. The maximum value $R_{//}$ and minimum value $R_\perp$ are corresponding to AMR when H is parallel and perpendicular to the direction of current, respectively. By changing the direction of applied field, the M follows the orientation of external field and the values of AMR show a periodically oscillated behavior. However, due to the magnetic anisotropy, M is no longer kept along with the external

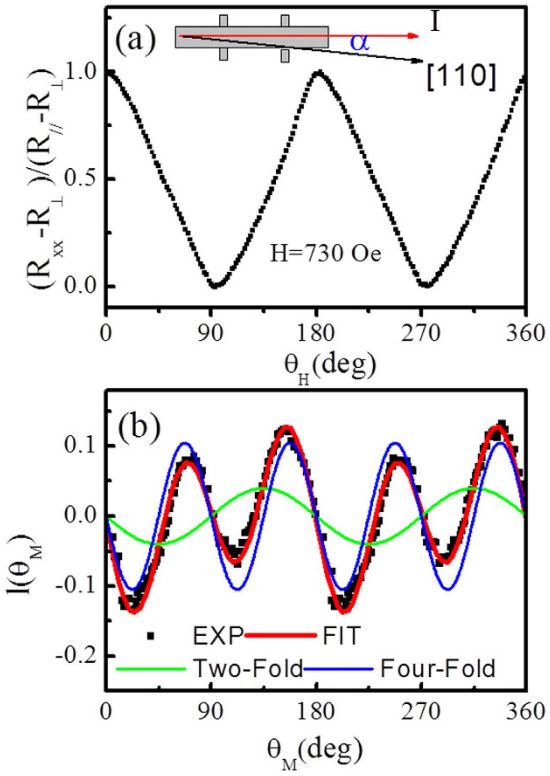

Figure 2. The in-plane AMR curve and the normalized magnetic torque curve. (**a**) The angular dependence AMR measurement at high field of 730 *Oe*, (**b**) The experimental and simulated normalized magnetic torque curves.

field H during rotation[22]. The AMR value is related to θ_M on basis of Eq. (1). The normalized magnetic torque $l(\theta_M) = L(\theta_M)/\mu_0 M_S H = \sin(\theta_H - \theta_M)$ can be obtained.

Since the applied field of 730 *Oe* is large enough to guarantee a single domain rotation in Fe/MgO(001) system, the total energy consisting of the magnetic anisotropy energy and Zeeman energy can be expressed as Eq. (2)[15].

$$E = K_U \sin^2(\theta_M) + \frac{K_1}{4}\cos^2(2\theta_M) - \mu_0 MH \cos(\theta_M - \theta_H) \tag{2}$$

In equilibrium state $\frac{\partial E}{\partial \theta_M} = 0$, the normalized magnetic torque is:

$$l(\theta_M) = \sin(\theta_M - \theta_H) = \left(-K_U \sin(2\theta_M) + \frac{K_1}{2}\sin(4\theta_M)\right)/\mu_0 MH \tag{3}$$

By fitting the magnetic torque curve by Eq. (3), which is shown in Fig. 2(b), $K_1 = 2.67 \times 10^4 J/m^3$ and $K_U = 4.2 \times 10^3 J/m^3$ can be obtained.

It can be observed from Fig. 2(b) that the magnetic torque shows a superposition of two- and four-fold magnetic anisotropies from the UMA constant K_U and the four-fold magnetic anisotropy constant K_1, respectively. The competition between K_1 and K_U leads to a slight deviation of easy magnetization axis about $\delta = \frac{1}{2}\sin^{-1}\left(\frac{K_U}{K_1}\right) = 4.5°$ from Fe[100] direction[9].

Figure 3 illustrates the angular dependence of AMR at different applied magnetic fields with clockwise (CW) and counterclockwise (CCW) rotations. The AMR curves at high magnetic field of 387 *Oe* shown in Fig. 3(a) indicate a smooth behavior without hysteresis between CW and CCW rotations, implying a coherent rotation of magnetization in this field. Similar with planar Hall effect in GaMnAs films[13,24,25], the AMR curves at low fields show abrupt transitions at certain angles with hysteresis between CW and CCW rotations, suggesting the presence of multi-domain structures. In order to investigate the domain structures, we focus on the abrupt transition regions (shaded regions) at low field $H = 5$ *Oe* in Fig. 3(c). The current is applied at an angle of 6.3° with respect to the Fe[110] direction to distinguish two components of magnetization along the two easy axes, which makes AMR reach minimum and maximum values when M is along $[\bar{1}00]$ and [010] directions, respectively. The AMR at low field of 5 *Oe* (Fig. 3(c)) is taken due to its quite plateau between two abrupt transitions, indicating that 90° domain nucleation

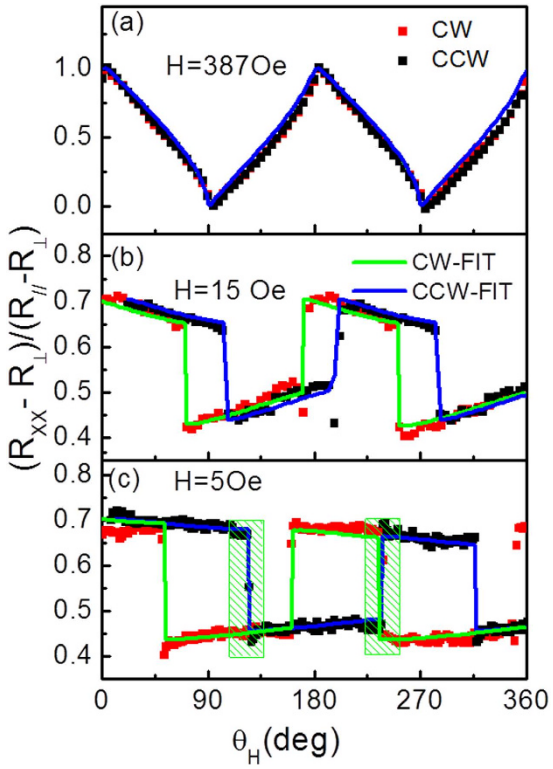

Figure 3. The experimental and fitting angular dependences of AMR data at different fields (**a**) 387 *Oe*, (**b**) 15 *Oe* and (**c**) 5 *Oe* with different rotation directions. The experimental data (red and black symbols) and the fitting data (green and blue solid line) are taken with field rotations in the clockwise (CW) and counter clockwise (CCW) directions.

and propagation, as observed by Kerr microscope and discussed in ref. 24. Under this low field, the direction of M switches from the Fe[010] direction to Fe[$\bar{1}$00] and Fe[$\bar{1}$00] to [0$\bar{1}$0]. The magnetization in this transition region can be calculated from $M_{near\,[\bar{1}00]} = (1-p)|M_H|$, where p is the fraction of $M_{[010]}$ as shown in inset of Fig. 4(a) [26]. According to Eq. (1), when M is near Fe[010] and Fe[$\bar{1}$00], AMR is in the high resistance state R_H (Eq. (4)), and the low resistance state R_L (Eq. (5)), respectively.

$$R_H = \Delta R\cos^2\left(\frac{\pi}{4} - \delta - \alpha\right) \tag{4}$$

$$R_L = \Delta R\cos^2\left(\frac{\pi}{4} - \delta + \alpha\right) \tag{5}$$

Therefore, in the intermediate state R_I can be expressed as Eq. (6).

$$\begin{aligned} R_I = \Delta R\cos^2(\theta_M - \alpha) = \Delta R\left[\cos\alpha + \sin\alpha \times \frac{1}{2p-1}\tan\left(\frac{\pi}{4} - \delta\right)\right]^2 \Big/ \\ \left\{\left[\cos\alpha + \sin\alpha \times \frac{1}{2p-1}\tan\left(\frac{\pi}{4} - \delta\right)\right]^2 \right. \\ \left. + \left[\cos\alpha \times \frac{1}{2p-1}\tan\left(\frac{\pi}{4} - \delta\right) - \sin\alpha\right]^2\right\} \end{aligned} \tag{6}$$

where $\theta_M = \arctan\left(\frac{1}{2p-1}\tan\left(\frac{\pi}{4} - \delta\right)\right)$, $\Delta R = R_{//} - R_{\perp}$, $\alpha = 6.3°$ and $\delta = 4.5°$. The values of p vs θ_H can be plotted in Fig. 4(a) according to Fig. 3(c) and Eq. (6).

On the other hand, the direction of M is also involved in the magnetic total energy E. The switching of M cross the [$\bar{1}$10] axis must overcome the energy between minima at [$\bar{1}$00] and [010][24]. This energy is then given by Eq. (2):

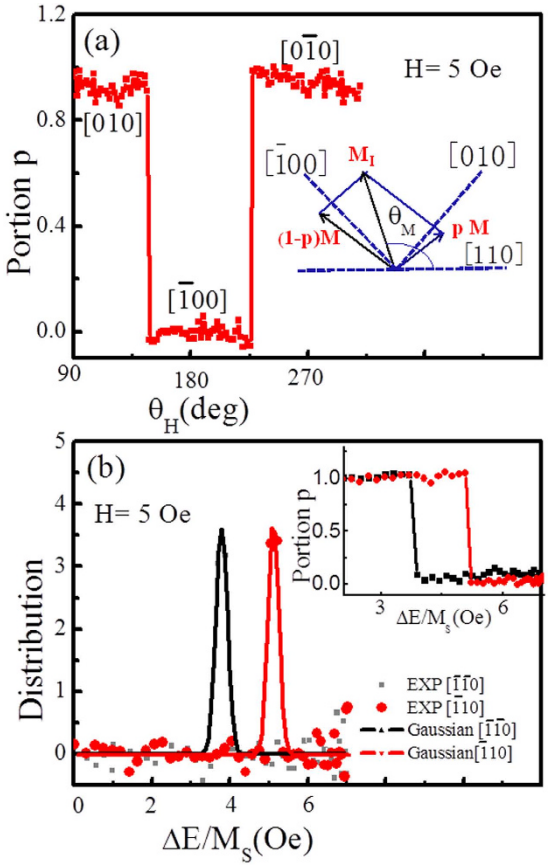

Figure 4. Probability of finding magnetic domains oriented along the [010] direction and the distributions of pinning fields. (**a**) The fraction p varying with magnetic flied direction and inset shows configuration of two magnetic domains for an intermediate state producing a resultant magnetization between two easy axes. (**b**) The distributions of pinning fields were obtained by derivative of p with respect to $\Delta E/M_s$. The relation between p and the pinning field $\Delta E/M_s$ for crossing two hard axes as shown in inset figure.

$$\Delta E_{[\bar{1}10]} = E_{[010]} - E_{[\bar{1}00]} = 2\mu_0 MH \cos\theta_H \sin[(\theta_M^{[010]} - \theta_M^{[\bar{1}00]})/2] \quad (7)$$

$$\Delta E_{[\bar{1}\bar{1}0]} = E_{[\bar{1}00]} - E_{[0\bar{1}0]} = 2\mu_0 MH \cos\theta_H \sin[(\theta_M^{[\bar{1}00]} - \theta_M^{[0\bar{1}0]})/2] \quad (8)$$

where $\Delta E_{[\bar{1}10]}$ is the energy difference between [010] and [$\bar{1}$00] transition; $\Delta E_{[\bar{1}\bar{1}0]}$ is the energy difference between [$\bar{1}$00] and [0$\bar{1}$0] transition. Since the energy difference ΔE varies as $H \cos\theta_H$ in Eqs. (7) and (8), it can be swept continuously by varying θ_H. This provides a direct handle for investigating the domain wall pinning energy distribution[10]. As the probed region in figure breaks up into two regions with the different components of M, the value of AMR can reflect the fractional areas corresponding to these two components in Fig. 4(a).

On basis of Eqs. (7) and (8), we can get the energy difference ΔE by varying θ_H. From Fig. 4(a) (p vs θ_H) and Eq. (7) (ΔE vs θ_H), the relationship between fraction p and ΔE is shown in the inset of Fig. 4(b). The black and red lines represents the switching from $M_{[010]}$ to $M_{[\bar{1}00]}$ and from $M_{[\bar{1}00]}$ to $M_{[0\bar{1}0]}$, respectively. The distributions of pinning fields were obtained by derivative of p with respect to $\Delta E/M_s$ as shown in Fig. 4(b), which can be fitted by a Gaussian function[24]. The domain wall pinning fields of 3.78 *Oe* and 4.5 *Oe* were obtained at [$\bar{1}\bar{1}$0] and [$\bar{1}$10], respectively. The difference in domain wall pinning fields at these two axes is related to the superimposed UMA along the [$\bar{1}\bar{1}$0] direction, which reduces the energy barrier for this direction.

From the analysis above, the magnetization switching process obeys coherent rotation model at high fields and domain nucleation and propagation at low fields. We investigate the AMR data at the different fields according to those two models in Fig. 3. At high field of 387 *Oe*, only coherent rotation model is used to calculate the AMR, which shows good agreement with experiment as shown in Fig. 3(a). At low

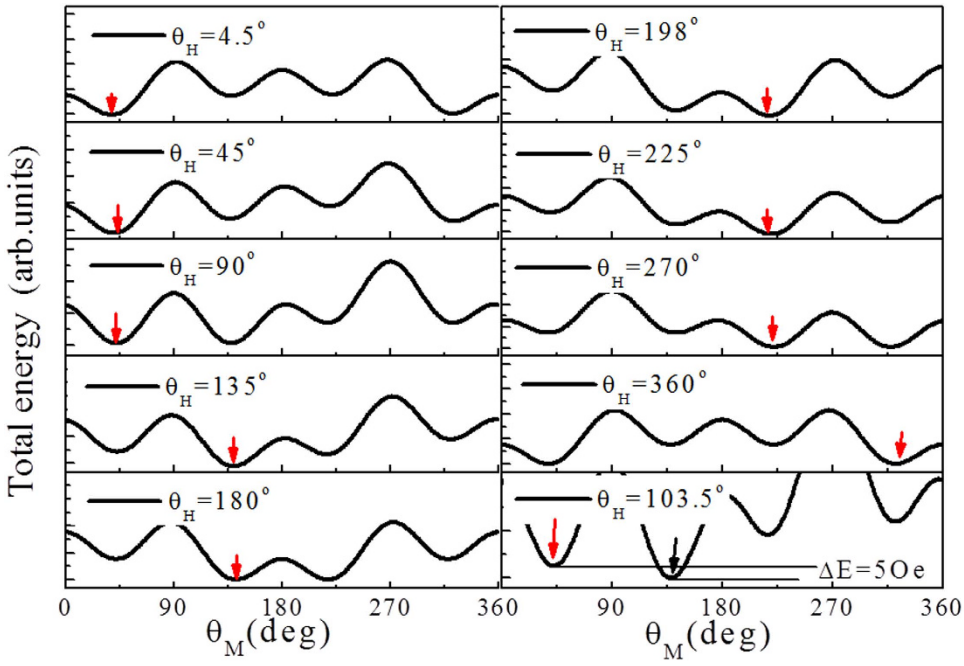

Figure 5. The evolution of magnetic total energy density with rotating field direction such as for H = 15 *Oe*. The solid red rows at the minima indicate the orientations of magnetization. Following the direction of the magnetic field rotating 360°, the direction of magnetic domains in the sample follows [010] → [$\bar{1}$00] →[0$\bar{1}$0] → [100] → [010] reorientation.

field of 5 *Oe*, the four stable plateau of AMR indicates that the domains nucleation and propagation dominates, and the fitting results by domain wall pinning energy are in agreement with the experimental values. When applied magnetic field is between the low field (5 *Oe*) and saturation field, the magnetization switching process involves the domain nucleation and propagation and part of coherent rotation. Due to slight deviation current, coherent rotation of magnetization at easy axis and propagation of domains between two easy axes are observed, which reflects in the tilted plateau and jump of AMR. The domain wall pinning and coherent rotation analysis as above were used to the fitting data at unsaturated fields. For $H = 15$ *Oe* as an example, the coherent rotation is dominated firstly. When the applied field rotates to a certain angle (103.5°) and energy differences between neighboring minima is larger than domain wall pinning energy, the near 90° domain switching appears. The K_U and K_1 obtained at high field and domain wall pinning field obtained at low field are used to fit the AMR of 15 *Oe*, which is the blue and green solid line shown in Fig. 3(b).

All the behavior of AMR can be explained by total energy density E given in Eq. (2), which includes four-fold anisotropy energy, UMA energy, and Zeeman energy. Figure 5 shows the variation of E at different direction of the fixed field $H = 15$ *Oe*. The four minima positions can be clearly observed. The solid red rows at the minima indicate the orientations of magnetization. The first panel at $\theta_H = 4.5°$ indicates that the entire sample is magnetized along a near Fe[010] direction. Following the direction of the magnetic field rotating 360°, the direction of magnetization in the sample follows [010] → [$\bar{1}$00] → [0$\bar{1}$0] → [100] → [010] orientation as shown in Fig. 5.

In contrast to the coherent rotation model, which means that the magnetization locates at the position of total energy minima, the magnetization position is actually not at energy minima in some values θ_H of unsaturation magnetic field. For $H = 15$ *Oe*, when $\theta_H = 103.5°$, the direction of magnetization is still at Fe[010] axis, but the minimum energy is at [$\bar{1}$00] direction. Therefore, the energy difference between two directions is domain wall pinning energy. Interestingly, the value of the domain wall pinning field governed the switching of Fe[010] → Fe[$\bar{1}$00], $\Delta E_{[\bar{1}10]}/M_S = 5$ *Oe*, is comparable with the experimental results.

Discussion

The magnetization switching process in Fe/MgO(001) film, which is dominated by both magnetic anisotropy energy and domain wall pinning energy, was investigated by AMR technique. In order to deduce magnetic anisotropy constants and domain wall pinning energy, the current is applied at an angle of 6.3° with respect to the hard axis (Fe[110]) direction) for AMR measurements. This configuration can distinguish the magnetization along the two easy axes and detect the small rotation of magnetization in easy axis direction. The AMR curves at magnetic fields high enough to ensure the coherent rotation of

magnetization indicate a smooth behavior without hysteresis between CW and CCW rotations. By analyzing magnetic torque, the values and orientations of K_U and K_1 can be confirmed. On the other hand, the AMR curves at low fields show abrupt transitions with hysteresis between CW and CCW rotations, suggesting the presence of multi-domain structures in the abrupt transition regions. When the applied field is far small than unsaturated field (~5 *Oe*), the domain wall pinning energy is obtained by analysis different behavior of AMR.

Methods

The Fe/MgO(001) film was prepared by molecular-beam epitaxy (MBE) in an ultrahigh vacuum (UHV) system with a base pressure of 2.0×10^{-10} *mbar*. After transferred into the UHV chamber, the MgO (001) substrate was first annealed at 700 °C for 2 hours to obtain clean surfaces. Fe film with thickness of 4.2 *nm* was grown at room temperature with a deposition rate 0.2 *nm/min*. Moreover, 4.5 *nm* Cu film was deposited on the Fe film as a capping layer to prevent sample from oxidization. The magneto-optical Kerr effect (MOKE) measurement was performed to confirm the magnetic properties. The angular dependence AMR measurements with a standard four-point method were carried out at room temperature and the details are described in ref. 14. The measuring time of one AMR point is far larger than magnetization switching time, and consequently the magnetization is always in equilibrium state during measurement. The current is applied at an angle of 6.3° with respect to the Fe[110]) direction to distinguish two components of magnetizations along the two easy axes.

References

1. Yuasa, S., Nagahama, T., Fukushima, A., Suzuki, Y. & Ando, K. Giant room-temperature magnetoresistance in single-crystal Fe/MgO/Fe magnetic tunnel junctions. *Nat. Mater.* **3,** 868–871(2004).
2. Bowen, M. *et al.* Large magnetoresistance in Fe/MgO/FeCo (001) epitaxial tunnel junctions on GaAs (001). *Appl. Phys. Lett.* **79,** 1655–1657 (2001).
3. Butler, W. H., Zhang, X. G. & Schulthess, T. C. Spin-dependent tunneling conductance of Fe/MgO/Fe sandwiches. *Phys. Rev. B* **63,** 054416 (2001).
4. Matsukura, F., Tokura, Y. & Ohno, H. Control of magnetism by electric fields. *Nat. Nanotechnol.* **10,** 209–220 (2015).
5. Zhao, H. B. *et al.* Interface Magnetization Reversal and Anisotropy in Fe/AlGaAs(001). *Phys. Rev. Lett.* **95,** 137202 (2005).
6. Chen, J. & Erskine, J. L. Surface step induced magnetic anisotropy in thin epitaxial Fe films on W(001). *Phys. Rev. Lett*. **68,** 1212–1215 (1992).
7. Park, Y., Fullerton, E. E. & Bader1, S. D. Growth-induced uniaxial in-plane magnetic anisotropy for ultrathin Fe deposited on MgO(001) by oblique-incidence molecular beam epitaxy. *Appl. Phys. Lett.* **66,** 2140–2142 (1995).
8. Daboo, C. *et al.* Anisotropy and orientational dependence of magnetization reversal processes in epitaxial ferromagnetic thin films. *Phys. Rev. B* **51,** 15964–15973 (1995).
9. Zhan, Q. F., Vandezande, S. & Haesendonck, C. V. Manipulation of in-plane uniaxial anisotropy in Fe/MgO(001) films by ion sputtering. *Appl. Phys. Lett.* **91,** 122510 (2007).
10. Zhan, Q. F., Vandezande, S., Temst, K. & Haesendonck, C. V. Magnetic anisotropies of epitaxial Fe/MgO(001) films with varying thickness and grown under different conditions. *New Journal of Physics* **11,** 063003 (2009).
11. Cowburn, R. P., Gray, S. J., Ferré, J., Bland, J. A. C. & Miltat, J. Magnetic switching and in-plane uniaxial anisotropy in ultrathin Ag/Fe/Ag(100) epitaxial films. *J. Appl. Phys.* **78,** 7210–7218 (1995).
12. Thomas, V. H. *et al.* Dual wavelength magneto-optical imaging of magnetic thin films. *Appl. Phys. Lett.* **103,** 142410 (2013).
13. Zheng, W., Hanbicki, A. T., Jonker, B. T. & Lüpke G. Control of magnetic contrast with nonlinear magneto-plasmonics. *Sci. Rep*. **4,** 6191 (2014).
14. Meng, H. & Wang, J. P. Spin transfer in nanomagnetic devices with perpendicular anisotropy. *Appl. Phys. Lett.* **88,** 172506 (2006).
15. Kim, J., Lee, H., Yoo, T. & Lee, S. Effect of pinning-field distribution on the process of magnetization reversal in $Ga_{1-x}Mn_xAs$ films. *Phys. Rev. B* **84,** 184407 (2011).
16. Ye, J. *et al.* Determination of magnetic anisotropy constants in Fe ultrathin film on vicinal Si(111) by anisotropic magnetoresistance. *Sci. Rep*. **3,** 2148 (2013).
17. Di Bona, A. Giovanardib, C. & Valeri, S. Growth and structure of Fe on MgO(001) studied by modulated electron emission. *Surf. Sci*. **498,** 193–201 (2002).
18. Postava, K., Jaffres, H., Schuhl, A., Nguyen Van Dau, F., Goiran, M. & Fert, A. R. Linear and quadratic magneto-optical measurements of the spin reorientation in epitaxial Fe films on MgO. *J. Magn. Magn. Mater.* **172,** 199–208 (1997).
19. Miller, B. H. & Dahlberg, E. D. Use of the anisotropic magnetoresistance to measure exchange anisotropy in Co/CoO bilayers. *Appl. Phys. Lett*. **69,** 3932–3934 (1996).
20. Krivorotov, I. N. Leighton, C., Nogués, J., Schuller, I. K. & Dahlberg, E. D. Relation between exchange anisotropy and magnetization reversal asymmetry in Fe/MnF_2 bilayers. *Phys. Rev. B* **65,** 100402 (2002).
21. Cao, W. N., Li, J., Chen, G., Zhu, J., Hu, C. R. & Wu, Y. Z. Temperature-dependent magnetic anisotropies in epitaxial Fe/CoO/MgO(001) system studied by the planar Hall effect. *Appl. Phys. Lett.* **98,** 262506 (2011).
22. Li, J. *et al.* Design of a vector magnet for the measurements of anisotropic magnetoresistance and rotational magneto-optic Kerr effect. *Rev. Sci. Instrum*. **83,** 033906 (2012).
23. Gruyters, M. Deviations from unidirectional anisotropy in layered exchange-bias systems due to breakdown of rigid spin rotations. *Phys. Rev. B* **73,** 014404 (2006).
24. Kim, J., Shin, D. Y. & Lee, S. Distribution of magnetic domain pinning fields in $Ga_{1-x}Mn_xAs$ ferromagnetic films. *Phys. Rev. B* **78,** 075309 (2008).
25. Chung, S., Lee, S., Liu, X. & Furdyna, J. K. Magnetization reorientation in $Ga_{1-x}Mn_xAs$ films: Planar Hall effect measurements. *Phys. Rev. B* **81,** 155209 (2010).
26. Chung, S. J., Shina, D. Y., Son, H., Lee, S., Liu, X. & Furdyna J. K. Time stability of multi-domain states formed in the magnetization reversal process of GaMnAs film. *Solid State Commun*. **143,** 232–235 (2007).

Acknowledgments

This work was supported by the National Basic Research Program of China (973 program, Grant Nos. 2015CB921403, 2011CB921801, and 2012CB933102), the National Natural Sciences Foundation of China (51427801, 11374350, and 11274361).

Author Contributions

Z.H.C., B.H., W.H. and J.Y. planned the experiments. B.H. carried out the experiments. J.T., Y.S.Z., S.S.A., and X.Q.Z. have some contributions for AMR and MOKE measurements. All the co-authors contributed to the analysis and discussion for the results. Z.H.C. and B.H. wrote the paper with the input from all the co-authors.

Additional Information

Competing financial interests: The authors declare no competing financial interests.

How to cite this article: Hu, B. *et al.* Determination of magnetic anisotropy constants and domain wall pinning energy of Fe/MgO(001) ultrathin film by anisotropic magnetoresistance. *Sci. Rep.* **5**, 14114; doi: 10.1038/srep14114 (2015).